INTERNATIONAL JOURNAL OF CIVIL ENGINEERING AND TECHNOLOGY (IJCIET)

ISSN 0976 – 6308 (Print)
ISSN 0976 – 6316(Online)
Volume 5, Issue 11, November (2014), pp. 154-164

Journal Impact Factor (2014): 7.9290 (Calculated by GISI)
www.jifactor.com

IJCIET

©IAEME

EXPERIMENTAL INVESTIGATION OF CONCRETE BEAMS REINFORCED WITH GFRP BARS

Ali S. Shanour[*1a], Ahmed A. Mahmoud[1b], Maher A. Adam[1c], Mohamed Said[1d]

[1]Department of Civil Engineering, Faculty of Engineering, Benha University, 108 Shoubra St., Shoubra, Cairo, Egypt

ABSTRACT

Glass fiber reinforced polymers (GFRP) reinforcement bars has a lower stiffness than steel reinforcement, which should be accounted for the ultimate and serviceability conditions, including the impact on member deflection and crack widths. This paper presents an experimental study of the flexural behavior of concrete beams reinforced with locally produced glass fiber reinforced polymers (GFRP) bars. The bars are locally produced by double parts die mold using local resources raw materials. A total of seven beams measuring 120 mm wide x 300 mm deep x 2800 mm long were caste and tested up to failure under four-point bending. The main parameters were reinforcement material type (GFRP and steel), concrete compressive strength and reinforcement ratio (μ_b, 1.7μ_b and 2.7μ_b). The mid-span deflection, crack width and GFRP reinforcement strains of the tested beams were recorded and compared. The test results revealed that the crack widths and mid-span deflection were significantly decreased by increasing the reinforcement ratio. The ultimate load increased by 47% and 97% as the reinforcement ration increased from μ_b to 2.7μ_b. Specimens reinforced by 2.7μ_b demonstrated an amount of ductility provided by the concrete. The recorded strain of GFRP reinforcement reached to 90% of the ultimate strains.

Keywords: Concrete Beams; Locally Produced; GFRP Bars; Deflection; Neutral Axis; Reinforcement Strain.

1. INTRODUCTION

The reinforced concrete structures suffering from corrosion of reinforcing steel problem. Steel reinforcement corrodes rapidly under aggressive conditions such as marine environments. The corrosion is caused by chloride ions, which can be found in de-icing salts in northern climates and sea water along coastal areas. Other materials, such as Fiber Reinforced Polymers (FRP), have emerged as an alternative to steel reinforcement when the exposure situation of the RC member requires durability under aggressive conditions. FRP materials are anisotropic and are characterized

by high tensile strength with no yielding only in the direction of the reinforcing fibers.The most common types of fibers are carbon, glass, and aramid. Glass Fiber Reinforced Polymers (GFRP) bars have linear stress-strain behavior under tension up to failure; however, they have lower modulus of elasticity and no ductility like the steel bars. Therefore FRP reinforcement is not recommended for moment resistance frames or zones where moment redistribution is required, (Raffaello, *et al.* 2007).

A number of studies (Benmokrane, *et al.* 1996, Pecce, *et al.* 2000, El-Salakawy, *et al.* 2002, and Yost, *et al.* 2003) experimentally investigated the flexural behavior of concrete members reinforced with glass fiber-reinforced polymer (GFRP) reinforcing bars. They are studied the variations in concrete strength f_c', reinforcement ratio ρ, FRP bars type, and shear span-depth ratio (a_v/d). analyzed the performance of the beams in terms of their load carrying capacity and found that beams reinforced with GFRP bars experienced 3 times larger deflection at the same load level compared with steel reinforced beam. In addition, (Balendran, *et al.* 2004), concluded that the ultimate strength of sand coated GFRP reinforced specimens was 1.4 -2.0 times greater than that of the mild steel reinforced specimens but exhibited a higher deflection.

This paper is aimed, firstly, to produce GFRP bars using the available raw material in the local market, secondly, to present results of an experimental study of concrete beams reinforced with locally produced GFRP bars in terms of the deflection behavior, cracking, and ultimate load carrying capacity. Three different amounts of GFRP reinforcement and two grades of concrete compressive strength were used for that purpose.

2. TEST PROGRAM

2.1 Manufacturing and Testing of Glass FRP Reinforcement Bars

The test program is a part of an extensive research project that was carried out to study the behavior of concrete beams reinforced with GFRP bars (Shanour, *2014*). The GFRP bars were locally manufactured using glass fiber roving. Double sets of plastic mold were manufactured at private workshop to manufacture 2.80m long GFRP bars with 12mm diameter. The GFRP ripped bar of 12mm diameter and double sets of plastic mold are shown in Fig. (1). The tensile stress of GFRP bars was determined as the average tensile strength of the GFRP bar specimens of diameter 12mm and was found to be 640 *M*Pa.

2.2 Test Specimens

Ten GFRP RC beams were designed as simple span, with an adequate amount of longitudinal and shear reinforcement to fail by either tensile failure by rupture of GFRP bars or crushing of concrete in the central zone. Additionally, one RC beam with similar amount of steel reinforcement to one type of the GFRP RC elements was tested as a control beam for comparison purposes. Two 8 mm GFRP rebar were used as top reinforcement to hold stirrups. Three different amounts of longitudinal reinforcement ratios (μ_b, $1.7\mu_b$ and $2.7\mu_b$; where μ_b is the reinforcement ratio at balanced condition based on Eq. 5-3, ECP 208 2005) and t different concrete grades (25 and 45 MPa) were used. The steel reinforced concrete beam was designed to behave with the same cracked stiffness as the GFRP RC element with concrete compressive strength of 25 MPa and reinforced with ratio of 2.7μb. The beam tests layout is detailed in Fig. (2).

Fig. 1: Ripped 12mm bars with Crescent shaped lugs and double sets of plastic mold

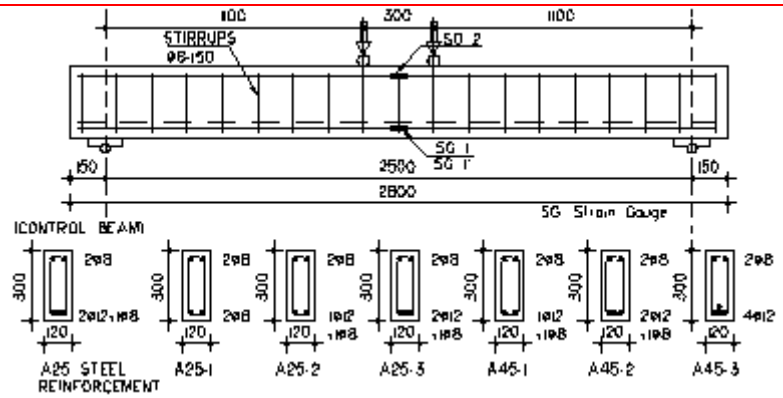

Fig. 2: Tested beams geometry and details

The tested beams details are summarized in Table 1. The beam types were identified as A-yy-z. The first term of the identification corresponded to a beams group. The second parameter identifies the beam series, characters 25 denoted that a target concrete strength of the series is 25 MPa, whilst 45 denoted that a target concrete strength of the series is 45 MPa. The last term indicates the specimen reinforcement, identification 1 for reinforcement ratio equal μ_b, identification 2 for reinforcement ratio equal $1.7\mu_b$, and identification 3 for reinforcement ratio equal $2.7\mu_b$.

Table 1: Detail of test beams

Series	Beam specimen	Beam Dimensions		Effective Span, L (mm)	f_{cu} (MPa)		Reinforcement Ratio (μ) %	Bottom Reinforcements (GFRP Bars)	Top Reinforcements (GFRP Bars)	Stirrups (steel)
		Width b(mm)	Depth t (mm)		Target	Actual				
A25	A25*	120	300	2500	25	24.5	0.92 %	2 φ 12 +1 φ 8	2 φ 8	8 @ 150
	A25-1	120	300	2500	25	24.5	μ_b	2 φ 8	2 φ 8	8 @ 150
	A25-2	120	300	2500	25	24.5	1.7 μ_b	1 φ 12 +1 φ 8	2 φ 8	8 @ 150
	A25-3	120	300	2500	25	24.5	2.7 μ_b	2 φ 12 +1 φ 8	2 φ 8	8 @ 150
A45	A45-1	120	300	2500	45	48	μ_b	1 φ 12 +1 φ 8	2 φ 8	8 @ 150
	A45-2	120	300	2500	45	48	1.7 μ_b	2 φ 12 +1 φ 8	2 φ 8	8 @ 150
	A45-3	120	300	2500	45	48	2.7 μ_b	4 φ 12	2 φ 8	8 @ 150

* Steel reinforced beam (control beam)

2.3 Test Setup

The specimens were tested under four-point bending, with 2500 mm effective span, and 1100 mm shear span, the distance between loads being 300 mm. Each specimen was supported on

roller assemblies and knife edges to allow longitudinal motion and rotation. Fig. (3) shows the test setup and instrumentations for tested specimen. Two linear variable differential transformers (LVDT) were installed horizontally at the center of the specimen in the constant moment region to measure the neutral axis depth. Electrical resistance strain gauges were applied to the GFRP bars to measure the strain during the tests. The strain gages, electrical pressure sensors, and (LVDTs) voltages were fed into the data acquisition system. Each specimen was loaded in 30 -70 increments. The cracks of the specimens were mapped and test observations were recorded during loading and at the time of failure. Fig. (4) shows the crack growth of specimen A25-3.

Fig. 3: Tested setup and instrumentation

Fig. 4: Crack growth of specimen A25-3

3. TEST RESULTS AND DISCUSSION

During the test, the beams were observed visually until the first crack appeared and the corresponding load was recorded. The first cracking load was also verified from the load deflection and load-strain relationships. Table 3 provides a summary of the key experimental results for all beam specimens. The average initial cracking load of series A25 beams is 10.55 kN. The cracking load is directly related to concrete tensile strength which, in turn, is a function of compressive strength, increasing the concrete compressive strength is expected to yield higher cracking loads. The average initial cracking load of the series A45 beams is 16.25 kN. The ratio of the average cracking load of the series A25 beams to that of the series A45 beams was 1.54. This ratio is close to the ratio between the square root of the average compressive strength of the series A25 beams and that of the series A45 beams, which was 1.4. Amr El-Nemr, *et al.* 2013, concluded similar ratios regarding the initial cracking loads for different concrete compressive strength.

3.1 Mode of Failure

The failure mechanism for each specimen is given in Table 3. The steel reinforcement control beam, failed in flexure by yielding of the steel bars. Concrete crushing was the most common failure mode, occurring in the specimens of over-reinforced section for glass fiber reinforced specimens. Tension failure in the GFRP reinforcement was characterized by the rupture of GFRP bars at the region of maximum bending moment, it occurs in all beams that are reinforced with GFRP ratio lower than or almost equal the balanced reinforcement ratio μ_b. Fig. (5) depicts two sample of concrete crushing and rupture of GFRP failure modes . The non-ductile behavior of GFRP reinforcement makes it suitable for a GFRP member to have compression failure by concrete crushing, which exhibits some warning prior to failure. This requires the GFRP members to be designed for over-reinforcement. Amr El-Nemr, *et al.* 2013, recorded the same mode of failure with respect to the balanced reinforcement ratio μ_b.

Table 3: Test results and failure modes

Series	Beam specimen	Reinforcement Ratio (μ) %	Initial cracking load, P_{CT} (kN)	Failure load, P_{EXP} (kN)	Failure modes [a]	Maximum Midspan Deflection (mm)
A25	A25	0.92 %	10.2	74.2	F.F	52
	A25-1	μb	10.2	45.9	G.R	84
	A25-2	1.7 μb	10.8	40.7	G.R	55 [b]
	A25-3	2.7 μb	10.9	75.2	C.C	90
A45	A45-1	μb	15.8	55.8	G.R	80
	A45-2	1.7 μb	15.4	81.9	C.C	85
	A45-3	2.7 μb	17.6	109.8	C.C	78

[a] C.C: Concrete Crushing, G.R: GFRP bars Rupture, F.F: Flexure Failure due to steel yield.
[b] Sudden rupture of 12mm diameter GFRP bar.

(a) Concrete crushing failure. (b) Rupture of GFRP reinforcement bars

Fig. 5: Modes of failure.

3.2 Crack Patterns

The cracks patterns for series A25 are depicted in Fig. (6), generally, the first cracks were vertical flexural cracks in the vicinity of the tension zone within and near the constant moment region at a load of about 10.55 kN. New cracks continued to form while existing ones propagated vertically toward the compression zone and small branches appear near lower tension surface up to approximately 60% of the maximum load. At higher loading stages, the rate of formation of new cracks significantly decreases. Moreover, the existing cracks grow wider, especially the first formed cracks, and splitting to small short cracks adjacent to the main GFRP bars. It was observed that the cracks located adjacent and/or near the vertical stirrups.

(a) Specimen A25

(b) Specimen A25-1

(c) Specimen A25-2

(d) Specimen A25-3

Fig. 6: Cracks pattern of Series A25 at failure

3.3 Crack Width

Fig. (7) reveals that the increasing of reinforcement ratio μ reduces the crack width. At a load of 40 kN, the crack width recorded values of 4.4mm, 2.7mm, and 1.2mm for beam A25-1, A25-1, and A25-3 respectively. While, the crack width is 2.1mm, 1.15mm, and 0.70mm for beam A45-1, A45-2, and A45-3 respectively. As shown in Fig. (7d); specimens with GFRP reinforcement ratio of μ_b, at a load of 40 kN, increasing in the concrete compressive strength from 25Mpa to 45Mpa exhibit reducing in the crack width by 52%.

CAN/CSA S8063 specified a service-limiting flexural crack width of 0.5 mm for exterior exposure (or aggressive environmental conditions) and 0.7 mm for interior exposure. In addition, ACI 440.1R6 recommends using CAN/CSA S8063 limits for most cases. On the other hand, because there is a direct relationship between the strain in the reinforcing bars and the crack width, ISIS14 specified a value of 0.002 as a strain limit in GFRP reinforcing bars to control crack width. At strain value of 0.002, the crack width for beam A25-1, A25-2 and A25-3 is measured 1.1mm, 0.4mm and 0.25 respectively. In addition, the crack width is recorded 0.45mm, 0.3mm and 0.25mm for beam A45-1, A45-2 and A45-3 respectively at strain of 0.002.

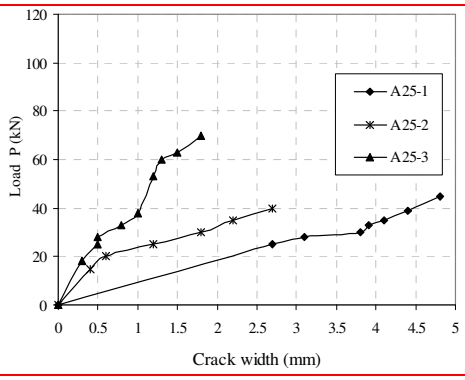

(a) Series A_{25}

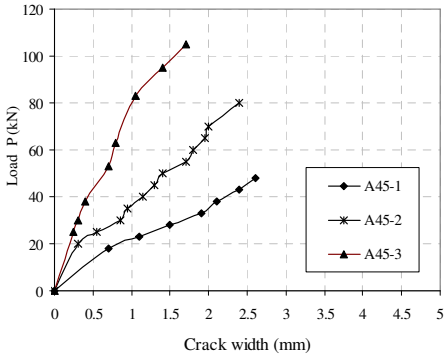

(b) Series A_{45}

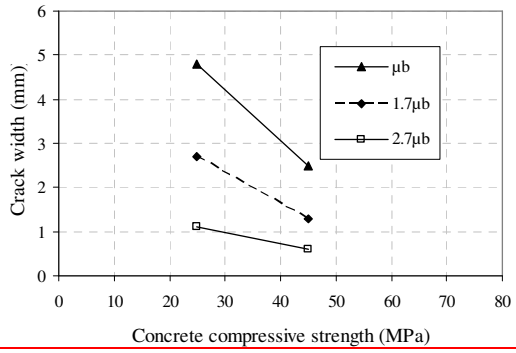

(c) Effect of concrete compressive strength

Fig.7: Crack width variation with load for different specimens

3.4 Load - Deflection Behavior

The experimental load to midspan deflection curves and failure loads of the steel and GFRP reinforced concrete beams are presented in Fig. (8) and Table 3. The first part of the curve up to cracking represents the behavior of the un-cracked beams. The second part represents the behavior of the cracked beams with reduced stiffness.

For the beams in series A25, the GFRP reinforced concrete beams A25-1, A25-2 and A25-3 exhibited greater midspan deflections than control steel reinforcement beam A25. Comparing the midspan deflection of specimens A25-3 and A25, at a given load level, larger deflection in the order of 2.6 to 4.8 times the deflection of the control specimen A25. This indicates that, for the same area of reinforcement, GFRP bars reveal different behavior than steel bars. For GFRP reinforced concrete beams, the midspan deflection decreased as the reinforcement ratio μ increased, similar conclusion has been introduced by Ilker and Ashour 2012. At 20 kN, the midspan deflections were 29.6, 20.3, and 11.2 mm for beams A25-1, A25-2, and A25-3, respectively. Fig. 8(a) reveals that increasing the reinforcement ratio from μ_b to $2.7\mu_b$, however, increases the ultimate capacity from 45.9 kN to 75.2 kN, giving an increase ratio of 1.63.

Fig. 8(b) shows the load to midspan deflection of series A45. As shown, at the deflection of 80 mm, the ultimate load of specimens A45-2 and A45-3 increased by 47% and 97% with respect to the ultimate load of specimen A45-1 respectively. At 31 kN, the midspan deflections were 34.5, 18.36, and 12.02 mm for beams A45-, A45-2 and A45-3, respectively.

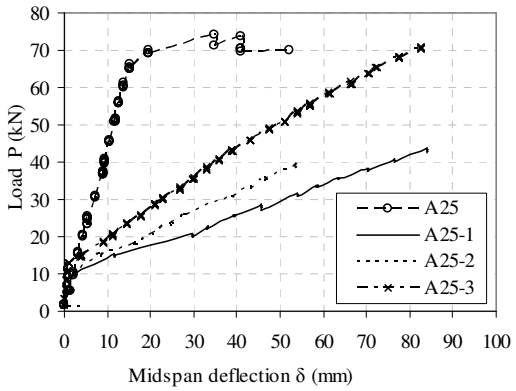

(a) Series A_{25}

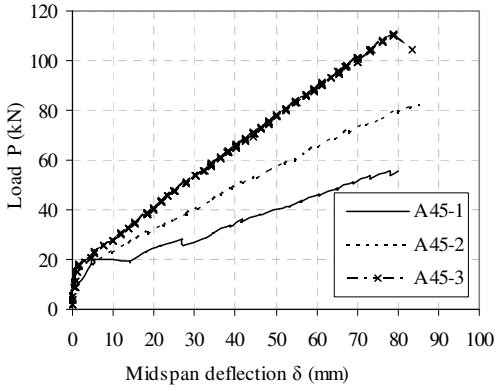

(b) Series A_{45}

Fig.8: Load–midspan deflection of tested beams

3.5 Concrete Strain at the Midspan Section

Using the data provided by the two transducers (LVDT) on the concrete surface at the midspan section as shown in Fig. (9), calculation of strains at upper and lower LVDT is carried out. The procedures are summarized in using linear interpolation, applying Bernoulli hypothesis, and then the experimental concrete strain at the extreme compressive fiber is deduced. The neutral axis depth was estimated in the basis of the upper and lower strain calculations for all the tested beams. Fig. (10) show the concrete strain evolution along the midspan section depth at different load stages for specimens A25-3 and A45-2, respectively.

The maximum compressive strain ε_{cu} was observed to range between 0.29% and 0.66%. These result values are higher than the usual ones established by (ACI Committee 318 2011, ACI Committee 440 2006) or (ECP 208, 2005), which consider ε_{cu} to be between 0.3% and 0.35% for the given concrete grades. (Abdul Rahman and Narayan 2005) obtained compressive strain ε_{cu} of 0.55% for concrete beams reinforced with GFRP bars. According to Cristina 2010, maximum compressive strain ε_{cu} was observed to be ranged between 0.4% and 0.55%, which agreed with the obtained results.

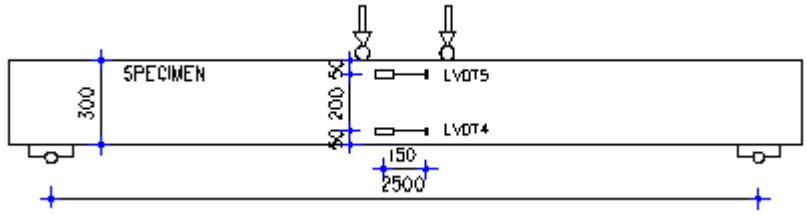

Fig. 9: Position of transducers (LVDT) on concrete at midspan section

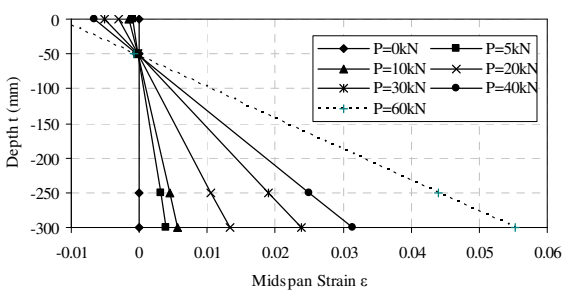

(a) Specimen A25-3

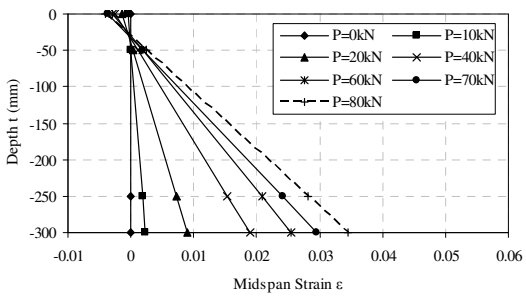

(b) Specimen A45-2

Fig. 10: Concrete strain evolution along the midspan depth

3.5.1 Neutral Axis Depth at the Midspan Section

The neutral axis depth increases with the reinforcement ratio, since equilibrium of forces requires a larger compression block for the greater forces arising from larger areas of reinforcement. For the same reinforcement ratio, specimens having higher concrete compressive strength possessed higher neutral axis depths. These observations are in agreement with the usual formulation to calculate the neutral axis position in the serviceability conditions in the absence of compression reinforcement.

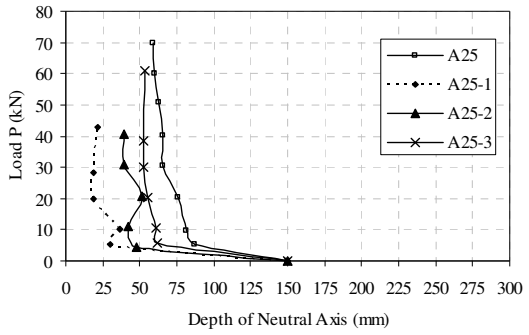

(a) Series A25

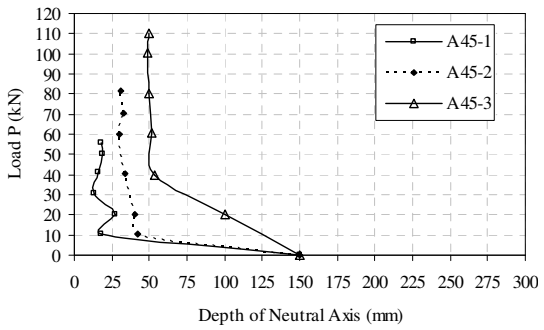

(b) Series A45

Fig. 11 Estimated neutral axis depth.

3.6 Strains in GFRP Reinforcement Bars

For all specimens there was a minimal change in the tensile GFRP reinforcement strain until the formation of the first flexural crack. The strain readings of the bottom bar increased rapidly in the vicinity of the first crack load, good agreement with the strain readings and the observation of first cracks was achieved. The strain distribution in the GFRP reinforcement bars of series A25and A45, with the load increased is shown in Fig. (12a and b), respectively.

The recorded tensile reinforcement strain for GFRP bars at near failure were in the range of 0.012 to 0.0177, these strains correspond to about 60% to 90% of the estimated ultimate strains of the GFRP bars obtained from the tensile test, which reached the value of 0.02. This indicates that rupture of GFRP bars were conducted for high values of tensile strain. However, the low values of tensile strain indicate that the GFRP bars did not rupture at the beam failure. On the other hand, for the control beam, the recorded steel bars strain was about 0.004 at yield and reach 0.0166 at the beam failure.

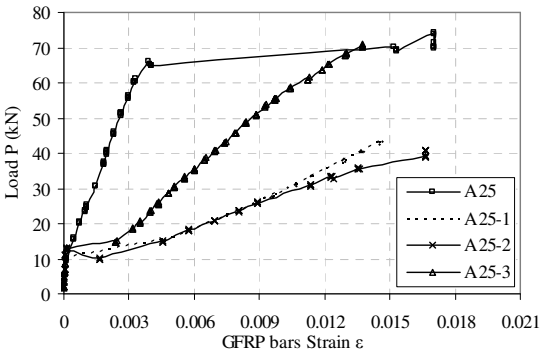

(a) Series A25

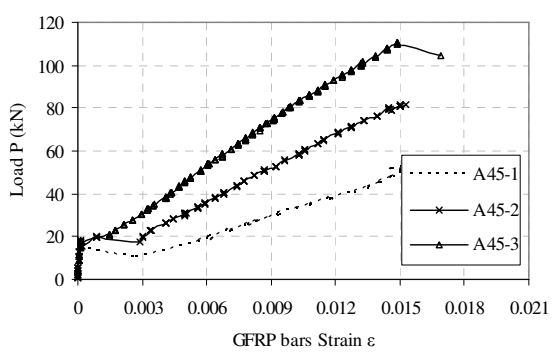

(b) Series A45

Fig. 12: Load- Strain in the GFRP reinforcement bars

4. CONCLUSIONS

Within the scope of this investigation and considering the materials used and comparison of the experimental results resulted in the following conclusions:

- The locally produced GFRP bars exhibit reasonable mechanical properties comparing with commercial products in terms of fiber volume fraction (70%), tensile strength (640 *M*Pa), and elastic modulus (30000 *M*Pa).
- The failure in GFRP RC beams reinforced with more than the balanced reinforcement μ_b was compression failure due to concrete crushing. While, Beams reinforced with GFRP ratio in order of lower than or almost equal the balanced reinforcement ratio μ_b exhibited rupture of GFRP reinforcement.
- Increasing the concrete compressive strength in the order of 25*M*pa to 45*M*pa exhibit reducing in the crack width by 52%.
- The loads deflection curves were bilinear for all GFRP reinforced beams. The first part of the curve up to cracking represents the behavior of the un-cracked beams. The second part represents the behavior of the cracked beams with reduced stiffness. Nevertheless, GFRP specimens with reinforcement ration, 2.7 µb, demonstrated that some amount of ductility can be provided.
- Increasing the reinforcement ratio from μ_b to $2.7\mu_b$, for series A25, increases the ultimate capacity from 45.9 kN to 75.2 kN respectively. giving an increase ratio of 1.63.
- The maximum concrete compressive strain ε_{cu} was recorded between 0.29% and 0.66%.
- The recorded tensile reinforcement strain for GFRP bars reached the range of 0.012 to 0.0177, these strains correspond to about 60% to 90% of the estimated ultimate strains of the GFRP bars obtained from the tensile test.

ACKNOWLEDGMENTS

The authors wish to acknowledge the financial support of the Civil Engineering Department, Faculty of Engineering Shoubra, Benha University, Cairo, Egypt. The first author is grateful of the chemical company BASF for supplied a free charge concrete admixtures.

REFERENCES

[1] Abdul Rahman M.S. and S. R. Narayan, (2005), "Flexural Behaviour of Concrete Beams Reinforced with Glass Fibre Reinforced Polymer Bars", *Jurnal Kejuruteraan Awam*, 17 (1), 2005. pp. 49-57.

[2] ACI Committee 440. (2003), ACI 440.1R-03, *Guide for the Design and Construction of Concrete Reinforced with FRP Bars*, American Concrete Institute (ACI), Farmington Hills, Mich., USA.

[3] ACI Committee 440 (2006), ACI 440.1R-06, *Guide for the Design and Construction of Concrete Reinforced with FRP Bars*, American Concrete Institute (ACI), Farmington Hills, Mich., USA.

[4] ACI Committee 318. (2011), *ACI 318R-05. Building Code Requirements for Structural Concrete (ACI 318-11) and Commentary (ACI 318R-11)*, American Concrete Institute (ACI), Farmington Hills, Mich., USA.

[5] Ali S. Shanour, (due 2014), "Behavior of Concrete Beams Reinforced with GFRP Bars", Ph.D. Dissertation, Faculty of Engineering, Shoubra, Benha University, Cairo, Egypt.

[6] Amr El-Nemr, Ehab A. Ahmed, and B. Benmokrane, (2013), "Flexural Behavior and Serviceability of Normal- and High-Strength Concrete Beams Reinforced with Glass Fiber-Reinforced Polymer Bars", *ACI Structural Journal*, **volume 110**, No. 6, November-December 2013.

[7] Balendran R.V., W.E. Tang, H.Y. Leung and A. Nadeem, (2004), "Flexural Behaviour of Sand Coated Glass-Fiber Reinforced Polymer (GFRP) Bars in Concrete", *29th Conference on* "*Our World in Concrete & Structures*", Singapore, August 2004.

[8] Benmokrane B., o. Chaallal, and R. Masmoudi, (1996), "Flexural Response of Concrete Beams Reinforced with FRP Reinforcing Bars", *ACI Structural Journal*, **volume 91**, No. 2, 1996, pp. 46-55.

[9] CAN/CSA S806–02, (2002), *Design and Construction of Building Components with Fibre Reinforced Polymers*, Canadian Standards Association, Rexdale, Ontario, Canada. 177pp.

[10] Cristina Barris P., Lluis Torres Llinas, (2010), "Serviceability Behaviour of Fibre Reinforced Polymer Reinforced Concrete Beams", PhD Thesis, University of Girona, Girona, Catalonia, Spain.

[11] ECP 208 (2005), *Egyptian Code of Practice for Design Principles of the Use of Fiber Reinforced Polymers in Construction*, Permanent Committee, Code No. 208, Cairo, Egypt.

[12] El-Salakawy E., Chakib Kassem, and Brahim Benmokrane, (2002), "Flexural Behaviour of Concrete Beams Reinforced with Carbon FRP Composite Bars", 4th Structural Specialty Conference of the Canadian Society for Civil Engineering Montréal, Québec, Canada, June 5-8, 2002.

[13] Ilker Fatih Kara, Ashraf F. Ashour, (2012), "Flexural Performance of FRP Reinforced Concrete Beams", *Journal of Composite Structures*, Available Online 29 December 2011.

[14] Raffaello F., Andrea P., Domenico A. (2007), "Limit States Design of Concrete Structures Reinforced With FRP Bars", PH.D. Thesis, University of Naples Federico, Naples, Italy.

[15] Pecce M., G. Manfredi, and E. Cosenza, (2000), "Experimental Response and Code Models of GFRP RC Beams in Bending", *ASCE, Journal of Composites for Construction*, **volume 4**, No. 4, November, 2000, pp. 182-190.

[16] Yost J. R., Gross S. P., And Dinehart D. W., (2003), "Effective Moment of Inertia for Glass Fiber-Reinforced Polymer-Reinforced Concrete Beams", *ACI Structural Journal*, **volume 100**, No. 6, 2003, pp. 732-739.

[17] Shaikh Zahoor Khalid and S.B. Shinde, "Seismic Response of FRP Strengthened RC Frame", *International Journal of Civil Engineering & Technology (IJCIET)*, Volume 3, Issue 2, 2012, pp. 305 - 321, ISSN Print: 0976 – 6308, ISSN Online: 0976 – 6316.

[18] A.S Jeyabharathy, Dr. S.Robert Ravi and Dr.G.Prince Arulraj, "Finite Element Modeling of Reinforced Concrete Beam Column Joints Retrofitted with GFRP Wrapping", *International Journal of Civil Engineering & Technology (IJCIET)*, Volume 2, Issue 1, 2011, pp. 35 - 39, ISSN Print: 0976 – 6308, ISSN Online: 0976 – 6316.